IRAQI JOURNAL OF APPLIED PHYSICS
IJAP, Vol. 10, No. 4, October-December 2014, pp. 15-19

Rashed T. Rasheed [(1)]
Sariya D. Al-Algawi [(2)]
Sahar Z. Tariq [(2)]

[(1)] *Applied Chemistry Division, School of Applied Sciences, University of Technology, Baghdad, Iraq*
[(2)] *Applied Physics Division, School of Applied Sciences, University of Technology, Baghdad, Iraq*

Preparation and Study of Indium Oxide Nanoparticles

In this study, In_2O_3 was prepared by reaction of indium acetate as precursor. The physical properties of the film were characterized by XRD, SEM, AFM, UV–visible thin film and FTIR spectroscopy measurements. The complete vibration analysis was carried out and the optimized parameters are calculated using DFT (B3LYP) method with 3-21G basis set for In_2O_3. A study of the electronic properties; absorption wavelengths, band gap energy, dipole moment, Kubo gap (HOMO and LUMO) and frontier molecular orbital energies, are performed by DFT method.

Keywords: Density functional theory, Formation energies, Electronic structure, Indium oxide
Received: 17/10/2014; **Revised**: 23/10/2014; **Accepted**: 30/10/2014

1. Introduction

In recent years, the properties and the applications of indium oxide nanostructures have been extensively studied. The very high surface to volume ratio can facilitate new and novel applications of indium oxide. A wide range of nano-sized powders has been synthesized to engineer desired properties such as chemical, electrical, mechanical and optical properties. Indium oxide (In_2O_3) material has recently attracted much attention due to its controversial basic material properties [1]. It exhibits a wide band gap (3.4-3.7) eV [2,3], and is a suitable candidate for the fabrication of various devices such as, field effect transistors, light emitting diodes, barrier layer in tunnel junctions [4-6], transparent conducting material in liquid crystal displays[7] photovoltaic (PV) and solar cells,[2] as well as a sensing material in gas sensors.[8,9]. One reason for this contradiction is the complex electronic band structure of In_2O_3 [10]. Many efforts have been made to understand structural, optical and electronic properties of indium oxide. There have been a great deal of research on synthesis and characterization of various nanostructured In_2O_3 [11]. Various methods have been used for the preparation of In_2O_3 powders and thin films [12-17]. It is generally known from literature reports [18] that nanostructured materials are influenced by shape, size and size distribution of small units, which in turn depend on the characteristics of synthesis. At the beginning of the line in the present work, In_2O_3 nanostructures were synthesized via Non-aqueous synthesis (aminolysis) method and its thin film by dipping method. The crystalline structure, morphology and particle size of the In_2O_3 were investigated using x-ray diffraction (XRD), SEM, AFM, UV–visible and FTIR spectroscopy measurements. The electrical properties of In_2O_3 nanostructures, thin film were also studied.

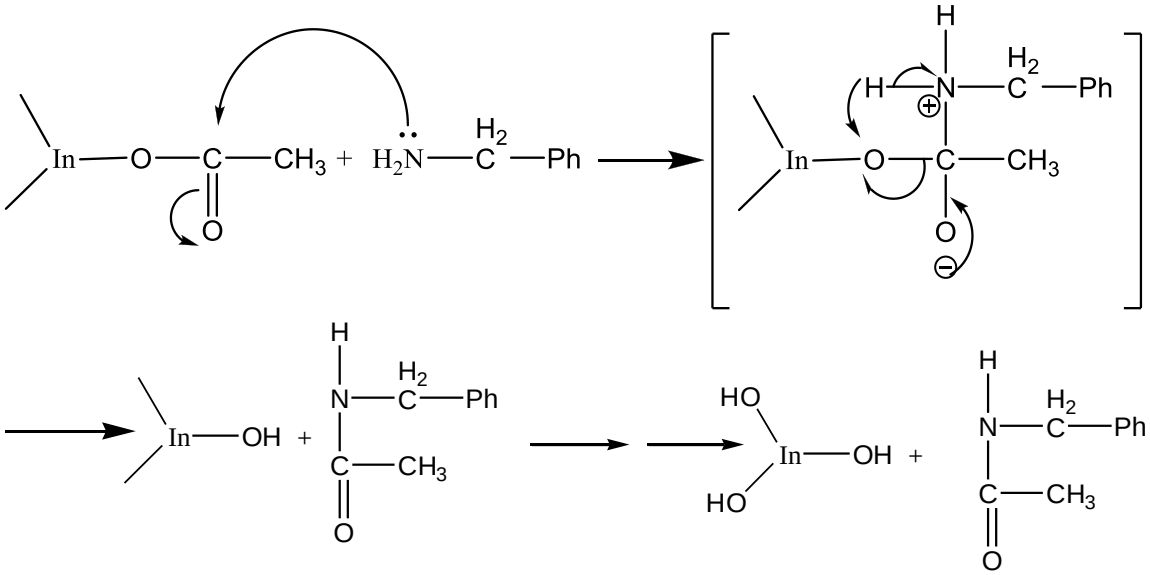

Scheme (1) Suggested mechanism of reaction between indium acetate and benzylamine

 ISSN (printed) 1813-2065, (online) 2309-1673 Printed in IRAQ

2. Experimental Procedure

Indium oxide was prepared by the non-aqueous synthesis (aminolysis) method by the reaction of indium acetate (1g) and benzylamine (20ml) to 180°C and maintained at this temperature for 3 hours. After reaction, white In $(OH)_3$ powder was separated through centrifugation, rinsed with ethanol two times, and dried in a vacuum oven at 90 °C for 12 h. The yellowish odorless powder of In_2O_3 (90%) was then cooled to room temperature. The suggested aminolysis mechanism is shown in Scheme (1).

The general reaction equation is:

$$In(CH_3COO)_3 + 3\,C_6H_5\text{-}CH_2NH_2 \rightarrow In(OH)_3 + 3\,C_6H_5\text{-}CH_2NHOCCH_3$$

$$2In(OH)_3 \rightarrow In_2O_3 + 3H_2O \qquad (1)$$

Thin film of In_2O_3 was prepared to study the UV-Visible only by using dipping method on a quartz slide substrate.

3. Computational Method

The geometrical optimization and the electronic structure calculation were conducted in the framework of density functional theory (DFT) through Becke's three parameter hybrid functional and Lee-Yang-Parr correlation functional (B3LYP) [19, 20] with 3-21G basis set. The structure analyzed in this study are fully optimized with the convergence criteria for an energy of 10^{-6} Hartree (1 Hartree = 27.21 eV). The vibrational frequencies of the lowest energy configurations are computed under harmonic approximation with the analytical force constants. All the calculations are performed by Gaussian 03 codes [21].

The highest occupied molecular orbital (HOMO) and the lowest unoccupied molecular orbital (LUMO) are important parameters to characterize the electronic stabilities of small clusters. The Koopmanns theory demonstrates that the HOMO energy level is associated with the cluster ability of losing its electrons, while the LUMO energy level equals to the electron affinity potential and reflects the cluster ability of obtaining the electrons. The LUMO-HOMO gap (E_g) determines the energy required by an electron hopping from the occupied orbital to unoccupied orbital. A large Egap means a higher energy required to perturb the electronic structure. The small cluster with a bigger Egap is more stable and possesses a weaker chemical activity.

4. Result and Discussion

It is well known that vibrational spectroscopy is a very useful technique for the determination of the crystal phase of In_2O_3. The FTIR spectrum of In_2O_3 nanopowder synthesized at the optimized preparation conditions is shown in Fig. (1).

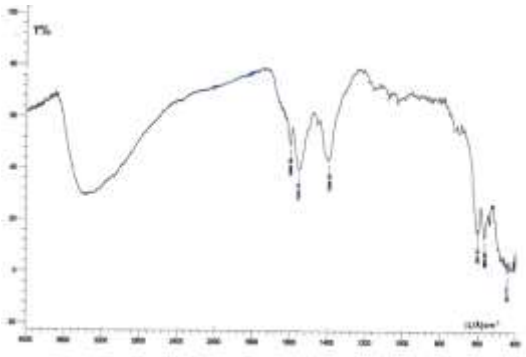

Fig. (1) FTIR spectrum of In_2O_3 nanoparticles

The band around 3400 cm^{-1} is attributed to the absorptions of hydroxyls from absorbing water or alcohols, because of the difficulty of removing the water residue completely. Three main intense peaks centered at 441, 583 and 601 cm^{-1} were observed, which is characteristic of the cubic In_2O_3 phase. According to the previous results reported in the literature, the observed bands at 441 and 583 cm^{-1} are attributed to In–O stretching in cubic In_2O_3 whereas the bands at 601 cm^{-1} is the characteristic of In–O bending vibrations in In_2O_3. Significantly, all the above bands have been reported in In_2O_3 [22]. The observed bands at 1595, 1552 and 1388 cm^{-1} are attributed to C=O, C-O or (C=C aromatic) and C-H (aromatic) respectively of residues benzylamine acetate.

Figure (2a) show the optical transmittance range 300-1000nm In_2O_3 thin film. The optical transmittance of the thin film is above 90% in the visible range. The optical absorption curve is located at about 300-400 nm. The absorption coefficients could be calculated from the transmission spectra in the UV region. Figure (2b) shows that the band gap of the film is 3.4 eV.

Figure (3a) shows the XRD pattern of the In_2O_3 nanoparticles, the stronger and sharper diffraction peaks in curves show that the In_2O_3 nanoparticles have a high degree of crystallization. The diffraction peaks agree with those given in JCPD data card of bulk cubic In_2O_3 reflections from (211), (222), (400) and (440) planes, The diffraction peaks show good crystalline nanoparticles and match very well with ideal lattice constants. The general morphologies of In_2O_3 nanoparticle were studied with scan electronic microscope (SEM) as shown in Fig. (3b). A mixed morphology with spherical and seeds shapes, the average size of nanoparticles is 77.24 nm.

 ISSN (printed) 1813-2065, (online) 2309-1673 Printed in IRAQ

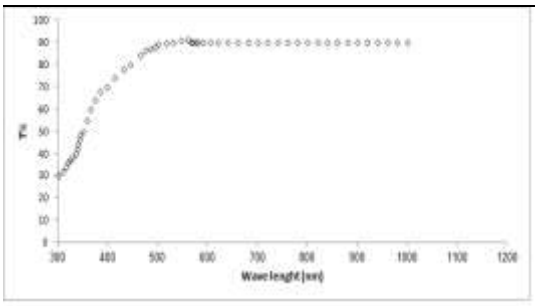

(a)

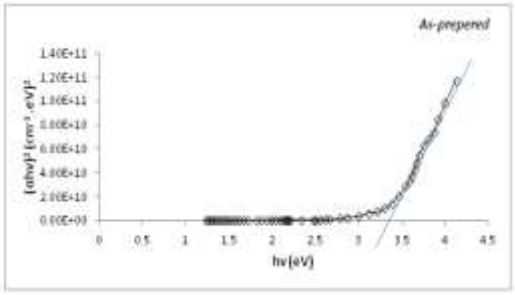

(b)

Fig. (2) (a) Optical transmission spectra and (b) band gap energy of In_2O_3 thin film

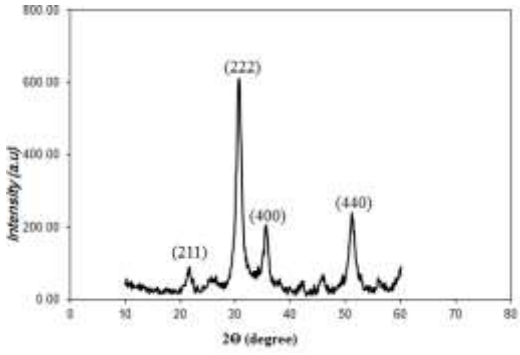

(a)

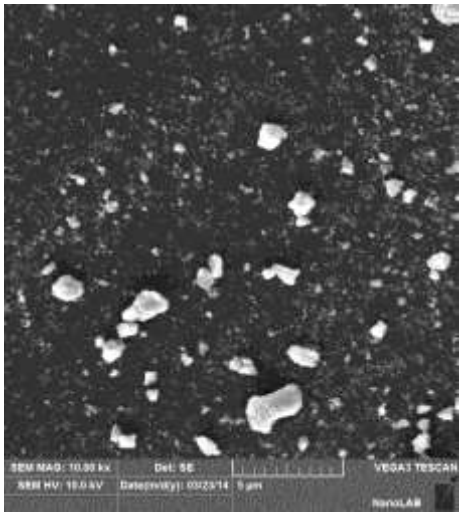

(b)

Fig. (3) (a) The XRD patterns and (b) scan electronic microscope of the In_2O_3 nanoparticles

Figure (4) shows a typical two and three dimensional atomic force microscope (AFM) images and the corresponding size distributions of the indium oxide nanoparticles as prepared. As shown in figure the better surface quality and crystallographic structure are obtained. It's clear from figure that In_2O_3 nanoparticles are spherical in shape, having average diameter of 72 nm are observed over the entire surface, this is in close agreement with SEM observation. The 3-dimensional (3D) AFM image of material nanoparticle in which the regular distributed In_2O_3 nanoparticles pillars and voids over the entire surface can be seen with a maximum value of 6.55 nm exhibits morphology with a root-mean-square (RMS) roughness of 0.634 nm.

The electron affinity (EA) and ionization potential (IP) are calculated for In_2O_3, in their most stable configurations. The definition of EA and IP we employed is as follows:

IP = - HOMO
EA = - LUMO

The electron affinity of ionic In_2O_3 (Fig. 4b) is found to be negative (EA=-0.36), and the ionization potential is found to be less positive (IP=0.066), when compared with neutral In_2O_3 (Fig. 4a) (EA=5.31, IP=6.15), which implies that the anionic In_2O_3 is more less stable as compared to the neutral one.

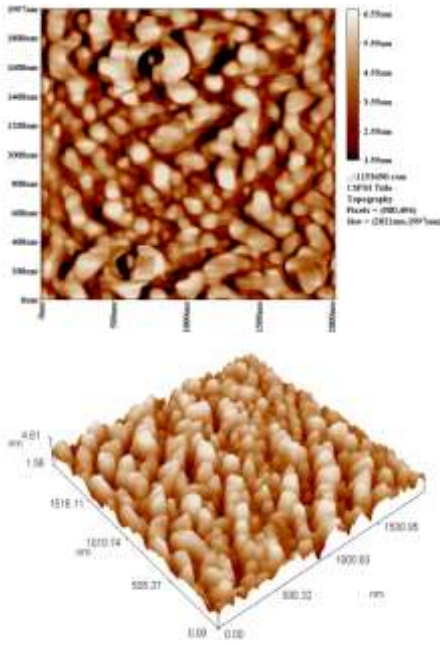

Fig. (4) AFM image of the prepared In_2O_3 nanoparticles

The optimized structure of indium oxide one unit (which has a neutral charge and singlet spin) and indium oxide (which has a negative charge and doublet spin) at ground state have symmetry of Cs and C_{2V} respectively (Fig. 4). The bond length and bond angles were calculated using DFT, B3LYP/3-21G (Table 1).

 ISSN (printed) 1813-2065, (online) 2309-1673 Printed in IRAQ

The LUMO–HOMO gaps (E-gaps) are calculated (see Table 2) for the neutral and anionic clusters of In_2O_3. The LUMO–HOMO gap is considered as the energy difference between the LUMO and HOMO irrespective of the fact that orbitals are of α-type or the β-type. It is noticeable that the gap depends on the ratio of indium and oxygen present in the cluster. It should be noted that the description of LUMO–HOMO gap may include the errors which inherently get introduced due to the usage of the hybrid functional [19].

From Table (2) the Egap is very low (0.84 eV) compared with its experimental results (3.6 e.V), this may be due to the theoretical results calculated only one unit, while experimental results calculated more than one (clusters).

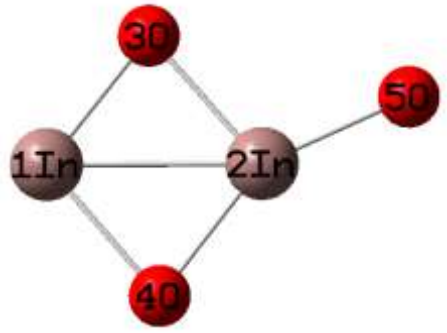

(a) Neutral form

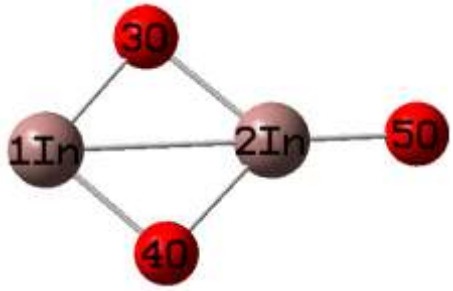

(b) Ionic form

Fig. (4) Optimized structure of one unit from indium oxide

5. Conclusions

Indium oxide nanoparticles were synthesized via a simple non-aqueous process using indium acetate as precursor. Structural, morphological and optical properties were investigated. The thin film transmission was above 90 % in the visible region, and the optical absorption curve is located at about 300 - 400 nm. Based on the XRD, SEM and AFM analyses, the current study shows that the size range of the nanoparticles is between (72–77 nm). DFT-B3LYP method with 3-21G basis set calculations has been applied to optimize the atomic equilibrium geometries and to study the stability of the two clusters (neutral and ionic). The neutral In_2O_3 cluster was found more stable than its ionic state.

References

[1] King P.D.C. et al., Band gap, electronic structure and surface electron accumulation of cubic and rhombohedral In_2O_3. Phys. Rev. 2009; 79 Suppl. 20:205211-205212.

[2] Tanaka I, Mizuno M and Adachi H., Electronic structure of indium oxide using cluster calculations. Phys. Rev. 1997; 56 Suppl. 15: 3536-33539.

[3] Fuchs F and Bechstedt F: Indium-oxide polymorphs from first principles, Quasi particle electronic states: Phys. Rev. 2008; 77 Suppl. 4: 55107-55109.

[4] Zhang D. et al., Diameter-controlled Growth of Single-crystalline In_2O_3 Nanowires and Their Electronic Properties Adv Mater. 2003: 15:143-145.

[5] Kim H. et al., Indium Tin Oxide Thin Films for Organic Light-Emitting Devices. Appl. Phys. Sci. Lett. 1999: 74 Suppl. 23:3444-3446.

[6] Kasiviswanathan S and Rangarajan G: Direct current magnetron sputtered In_2O_3 films as tunnel barriers. J. Appl. Phys. 1994; 75; 2572–2577.

[7] Falcony C. et al., Electroluminescence from indium oxide and indium-tin oxide. J. Appl. Phys. 1985; 58:3556-3558.

[8] Mane R S, Pathan HM, Lokhande CD, and Han SH: An Effective Use of Nanocrystalline CdO Thin Films in Dye-Sensitized Solar Cells. Solar Energy 2006; 80 Suppl. 2:185-190.

[9] Zhang D.H. et al., Detection of NO_2 down to ppb levels using individual and multiple In_2O_3 nanowire devices. Nano. Lett. 2004; 4:1919–1924.

[10] Wang C.Y. et al., NO"x sensing properties of In_2O_3 nanoparticles prepared by metal organic chemical vapor deposition, Sensors and Actuators 2008:130 Suppl. 2:589-593.

[11] Karazhanov S.Z. et al., Phase stability, electronic structure and optical properties of indium oxide polytypes. Phys. Rev. 2007; 76:75129-75131.

[12] Lin SE and Wei W C J: Synthesis and Investigation of Submicrometer Spherical Indium Oxide Particles. J. Am. Ceram. Soc. 2008; 91 Suppl. 4;1121-1128.

[13] Murali A. et al., Synthesis and Characterization of Indium Oxide Nanoparticles. Nano. Lett. 2001; 1:287-289.

[14] Seo WS, Jo HH, Lee K and Park JT: Preparation and Optical Properties of Highly Crystalline, Colloidal, and Size-Controlled Indium Oxide Nanoparticles. Adv. Mater. 2003; 15 Suppl. 10:795-797.

[15] Chu DYP, Zeng DJ and J Xu: Tuning the phase and morphology of In_2O_3 nanocrystals via

 ISSN (printed) 1813-2065, (online) 2309-1673 Printed in IRAQ

simple solution routes. Nanotechnology. 2007; 18 Suppl. 43: 5605-5609.
[16] Zhao Y, Wu AZ, and Dang H: Synthesis and characterization of single-crystalline In_2O_3 nanocrystals via solution dispersion. Langmuir. 2004; 6 Suppl.1:27-29.
[17] Rey J.F.Q. et al., Synthesis of In_2O_3 nanoparticles by thermal decomposition of a citrate gel precursor. J. Nanopart. Res. 2005; 7 Suppl. 2:203-208.
[18] Matsumoto T. et al., Evidence of quantum size effect in nanocrystalline silicon by optical absorption. Phys. Rev. 2001; 63:195322.
[19] Becke A.D., Density-functional thermochemistry. III: The role of exact exchange, J. Chem. Phys. 1993; 98:5648-5651.
[20] Lee C, Yang W and Parr RG: Development of the Colle-Salvetti correlation-energy formula into a function of the electron density. Phys. Rev. 1988; 37 Suppl. 2:785-789.
[21] Frisch M.J. et al., Gaussian 03, Revision C.02. Gaussian, Inc., Wallingford, Connecticut (2004).
[22] Souza E.C.C., Rey J.F.Q., Muccillo E.N.S., Synthesis and characterization of spherical and narrow size distribution indium oxide nanoparticles, Appl. Surf. Sci. 2009; 255 Suppl. 6:3779–3783.

Table (1a) Geometry properties of In_2O_3 in both (a) and (b) forms as in Fig. (4)

Compound	Charge	Symmetry	Dipole Moment (Debye)	Bond length between atoms (Å)					
				1-2	1-3	1-4	2-3	2-4	2-5
(a)	0	Cs	5.30	2.876	2.227	2.329	2.293	2.260	2.160
(b)	-1	C_{2V}	4.79	2.974	2.033	2.033	2.083	2.083	1.909

Table (1b) Geometry properties (angles) of In_2O_3 in both (a) and (b) forms as in Fig. (4)

Compound	Bond angle (Degree) between atoms					
	<314	<324	<132	<142	<325	<425
(a)	101.688	101.565	79.149	77.596	106.200	152.233
(b)	88.822	86.158	92.509	92.509	136.920	136.920

Table (2) Theoretical prosperities of In_2O_3 one unite calculated using DFT, B3LYP/3-21G

Compound	HOMO (eV)	LUMO (eV)	E_{gap} (eV)	Total Energy	Symmetry
(a)	-6.15	-5.31	0.84	-11659.507	Cs
(b)	-0.66	0.36	1.02	-11659.702	C_{2V}

 ISSN (printed) 1813-2065, (online) 2309-1673 Printed in IRAQ